IEEE Access
Multidisciplinary | Rapid Review | Open Access Journal

Received January 17, 2019, accepted January 29, 2019, date of publication February 1, 2019, date of current version February 22, 2019.

Digital Object Identifier 10.1109/ACCESS.2019.2896983

An Improved Complex-Valued Recurrent Neural Network Model for Time-Varying Complex-Valued Sylvester Equation

LEI DING[1], LIN XIAO[2], KAIQING ZHOU[1], YONGHONG LAN[3], YONGSHENG ZHANG[1], AND JICHUN LI[4], (Member, IEEE)

[1]College of Information Science and Engineering, Jishou University, Jishou 416000, China
[2]College of Information Science and Engineering, Hunan University, Changsha 410082, China
[3]College of Information and Engineering, Xiangtan University, Xiangtan 411100, China
[4]School of Science, Engineering and Design, Teesside University, Middlesbrough TS1 3BX, U.K.

Corresponding author: Lin Xiao (xiaolin860728@163.com)

This work was supported in part by the National Natural Science Foundation of China under Grant 61866013, Grant 61503152, Grant 61573298, Grant 61473259, and Grant 61562029, in part by the Hunan Provincial Science and Technology Project Foundation under Grant 2018TP1018, Grant 2018RS3065, and Grant 13C754, in part by the Open Fund Project of Hunan Engineering laboratory under Grant DNGC1703, and in part by the Scientific Research Fund of Hunan Provincial Education Department under Grant 17A173.

ABSTRACT Complex-valued time-varying Sylvester equation (CVTVSE) has been successfully applied into mathematics and control domain. However, the computation load of solving CVTVSE will rise significantly with the increase of sampling rate, and it is a challenging job to tackle the CVTVSE online. In this paper, a new sign-multi-power activation function is designed. Based on this new activation function, an improved complex-valued Zhang neural network (ICZNN) model for tackling the CVTVSE is established. Furthermore, the strict proof for the maximum time of global convergence of the ICZNN is given in detail. A total of two numerical experiments are employed to verify the performance of the proposed ICZNN model, and the results show that, as compared with the previous Zhang neural network (ZNN) models with different nonlinear activation functions, this ICZNN model with the sign-multi-power activation function has a faster convergence speed to tackle the CVTVSE.

INDEX TERMS Zhang neural network, complex-valued time-varying Sylvester equation, convergence speed, sign-multi-power function, finite-time convergence.

I. INTRODUCTION

Today the Sylvester equation (SE) has been successfully applied into many fields, such as the robotic application [1], the waveguide eigenvalue problem [2], the commutative rings [3], the isogeometric preconditioners [4], the multi-agent linear parameter-varying systems [5]. Generally speaking, the Sylvester equation can be divided into two categories: namely the static SE and the dynamic SE (i.e., time-varying Sylvester equation, TVSE). The classical algorithms to tackle the static SE are the Bartels−Stewart and Hessenberg−Schur methods [6], [7]. The main shortcoming of the above algorithms is that they only fit for solving the small-scale problems due to the dense matrix operation. Recently, a series of iteration algorithms using the gradient information have been proposed to tackle the static SE, such as the relaxed gradient based iterative algorithm [8], the least-squares iterative algorithm [9], the accelerated gradient algorithm [10], and the alternating direction implicit algorithm [11]. However, the above methods can not effectively tackle the TVSE online. The main reason is that the TVSE should be calculated in every sampling cycle, and the computational burden will significantly increase within a sampling cycle when the sampling rate increases. Thus the above algorithm may not complete a calculation if the computational burden is too big. Today the neural networks have caused widely attention [12]–[14]. As a kind of neural network, the recurrent neural networks (RNNs) have a stronger real-time computation ability than the traditional numerical algorithms [15]–[21]. So a series of RNN models have been designed for tackling the dynamic SE. For example, the gradient-based RNNs are designed to tackle the real-valued SE [22], [23]. But the

The associate editor coordinating the review of this manuscript and approving it for publication was Yan-Jun Liu.

gradient-based RNNs may need very long time to obtain its ideal solution because its performance indicator is the Frobenius norm of errors. So a novel RNN called Zhang neural network (ZNN), which can converge to zero exponentially, is proposed because its performance indicator is a vector/matrix-valued error function [24]–[29], [33]. But Xiao pointed [30] out that the traditional ZNN cannot obtain its theoretical solution in finite time. So a series of improved ZNNs with the finite time convergence property have been proposed [31]–[33]. Furthermore, some of improved ZNNs have been successfully employed to tackle the TVSE online [1], [34], [35].

Now the complex-valued neural networks have shown more advantages than the real-valued neural networks in some fields, such as the high-capacity auto-associative memories [36], the spectral domain [37], the millimeter-wave active imaging [38], and the geometric measures [39]. Inspired by the previous studies for the ZNNs, we explore a novel complex-valued ZNN model for solving the complex-valued time-varying Sylvester equation (CVTVSE) in this paper. Before that, some related work about complex-valued ZNNs is reviewed as follows. In [40], a ZNN model is applied to tackle a complex matrix inversion. However, a linear activation function is used in this ZNN model, which causes this ZNN model cannot obtain its ideal solution in finite time. Li *et al*. [41] proposed a novel sign-bi-power nonlinear activation function to build an improved ZNN model, which can obtain its theoretical results in finite time for tackling the TVSE. We can describe this sign-bi-power function as

$$\Psi(u) = \frac{1}{2}\mathrm{sgn}^z(u) + \frac{1}{2}\mathrm{sgn}^{1/z}(u), \tag{1}$$

where z is an odd integer and satisfy $z > 1$, and

$$\mathrm{sgn}^z(u) = \begin{cases} |u|^z, & \text{if } u > 0 \\ 0, & \text{if } u = 0 \\ -|u|^z, & \text{if } u < 0. \end{cases}$$

Furthermore, Li *et al*. [42] proposed a complex-valued ZNN based on the sign-bi-power function to tackle the CVTVSE. Inspired by the sign-bi-power function, a tunable activation function is designed to obtain a higher convergence rate in [43]. Ding *et al*. [44] designed an improved ZNN activation function to tackle the complex-valued linear equations (CVLE), which is transformed into a real-valued linear equation, and the improved ZNN activation function can be described as

$$\Psi(u) = \mathrm{sign}(u)(j_1|u|^h + j_2|u|^{1/h} - j_3|u|), \tag{2}$$

where $j_1 > j_3 > 0$, $j_2 > j_3 > 0$, h is an odd integer and satisfies $h > 1$, and

$$\mathrm{sign}(u) = \begin{cases} 1, & \text{if } u > 0 \\ 0, & \text{if } u = 0 \\ -1, & \text{if } u < 0. \end{cases}$$

According to the above idea, to obtain a higher convergence rate for online solving the CVTVSE, an improved nonlinear activation function is designed and investigated in this paper. Based on this new activation function, an improved complex-valued Zhang neural network (ICZNN) model for tackling the CVTVSE is established. Furthermore, the strict proof for the maximum time of global convergence of the ICZNN is given in detail. Two numerical experiments are employed to verify the performance of the proposed ICZNN model.

The remaining parts contain the following content. In Section II, we give the description of the problem. In Section III, we design a sign-multi-power function to build a novel ICZNN to tackle the CVTVSE, and give the theoretical proof for the maximum time of global convergence of the ICZNN. In Section IV, we give two digit experiments to verify the superiority of the sign-multi-power function. Finally, we give the final conclusions of this paper in Section V.

Before finishing this section, we can summarize the contribution of this paper as below.

1) A novel sign-multi-power activation function is designed.
2) A novel ICZNN is derived to tackle the CVTVSE in complex-valued domain, and the strict theoretical proof is explained.
3) The digit experiments demonstrate that this novel model for online tackling the CVTVSE can increase the convergence rate significantly.

II. DESCRIPTION OF THE PROBLEM

The CVTVSE can be described as

$$G(t)X(t) - X(t)Q(t) = -S(t) \in \mathbb{C}^{n\times n}, \tag{3}$$

where $G(t)$, $Q(t)$ and $S(t)$ are all the complex-valued coefficient matrices, t means time, and $X(t)$ is a time-varying matrix needs to be calculated. Now we give the following assumptions: the complex-valued matrices $G(t)$, $Q(t)$, and $S(t)$ have no identical eigenvalues, and are all first-order differentiable. So there will be only a solution for the equation (3). To help the future description, let $\tilde{X}(t)$ denote the theoretical solution. Our target is to design a novel nonlinear complex-valued activation function to build a neural network for tackling the CVTCSE.

First suppose $G(t)$, $Q(t)$, $X(t)$ and $S(t)$ are all real-valued matrices, and the procedure for the real-valued TVSE using the ZNN model can be described as the following three steps.

Step 1: The error function can be represented as:

$$D(t) = G(t)X(t) - X(t)Q(t) + S(t). \tag{4}$$

Step 2: The evolution procedure is designed as follows:

$$\dot{D}(t) = q\Psi(D(t)), \tag{5}$$

where $q > 0$ denotes the coefficient to accelerate the convergence rate, and $\Psi(\cdot)$ denotes the activation function.

Step 3: Substitute (4) into (5), and we will have the following equation:

$$\begin{aligned} &G(t)\dot{X}(t) - \dot{X}(t)Q(t) \\ &\quad = q\Psi(G(t)X(t) - X(t)Q(t) \\ &\qquad + S(t)) - \dot{G}(t)X(t) + X(t)\dot{Q}(t) - \dot{S}(t). \end{aligned} \tag{6}$$

Now suppose $G(t) = G_{\mathrm{re}}(t) + jG_{\mathrm{im}}(t)$, $Q(t) = Q_{\mathrm{re}}(t) + jQ_{\mathrm{im}}(t)$, $X(t) = X_{\mathrm{re}}(t) + jX_{\mathrm{im}}(t)$ and $S(t) = S_{\mathrm{re}}(t) + S_{\mathrm{im}}(t)$, where $j = \sqrt{-1}$ denotes an imaginary unit. Then according to the equation (6), we have

$$\begin{aligned} G(t)\dot{X}(t) - \dot{X}(t)Q(t) = q(&\Psi(G_{\mathrm{re}}(t)X_{\mathrm{re}}(t) \\ &- G_{\mathrm{im}}(t)X_{\mathrm{im}}(t) - X_{\mathrm{re}}(t)Q_{\mathrm{re}}(t) \\ &+ X_{\mathrm{im}}(t)Q_{\mathrm{im}}(t)) + j\Psi(G_{\mathrm{im}}(t)X_{\mathrm{re}}(t) \\ &+ G_{\mathrm{re}}(t)X_{\mathrm{im}}(t) - X_{\mathrm{im}}(t)Q_{\mathrm{re}}(t) \\ &- X_{\mathrm{re}}(t)Q_{\mathrm{im}}(t))) - \dot{G}(t)X(t) \\ &+ X(t)\dot{Q}(t) - \dot{S}(t). \end{aligned} \tag{7}$$

III. A NOVEL RECURRENT NEURAL NETWORK

A. A NEW NONLINEAR ACTIVATION FUNCTION

From the equation (7), we can find that a suitable activation function will increase the convergence rate significantly. So a novel nonlinear activation function called the sign-multi-power function can be designed as follows:

$$\begin{aligned} \Psi(k) = a_1\mathrm{sgn}^z(k) + a_2\mathrm{sgn}^{z-2^1}(k) + a_3\mathrm{sgn}^{z-2^2}(k) \\ + \cdots + a_n\mathrm{sgn}^1(k) + a_{n+1}\mathrm{sgn}^{1/z}(k), \end{aligned} \tag{8}$$

where z is odd integer and satisfy $z > 1$, the parameters a_1, $\cdots$, a_{n+1} are all the positive numbers, and

$$\mathrm{sgn}^z(u) = \begin{cases} |u|^z, & \text{if } u > 0 \\ 0, & \text{if } u = 0 \\ -|u|^z, & \text{if } u < 0. \end{cases}$$

B. A SIGN-MULTI-POWER MODEL FOR TACKLING THE CVTVSE

For ease of comparison, we first introduce two improved ZNN models. One is a sign-bi-power model [42], and the other is an IZNN model [44]. For ease of description, we first give the following definition:

$$\begin{aligned} f_1(t) = G_{\mathrm{re}}(t)X_{\mathrm{re}}(t) - G_{\mathrm{im}}(t)X_{\mathrm{im}}(t) \\ - X_{\mathrm{re}}(t)Q_{\mathrm{re}}(t) + X_{\mathrm{im}}(t)Q_{\mathrm{im}}(t), \end{aligned}$$

and

$$\begin{aligned} f_2(t) = G_{\mathrm{im}}(t)X_{\mathrm{re}}(t) + G_{\mathrm{re}}(t)X_{\mathrm{im}}(t) \\ - X_{\mathrm{im}}(t)Q_{\mathrm{re}}(t) - X_{\mathrm{re}}(t)Q_{\mathrm{im}}(t). \end{aligned}$$

Then the sign-bi-power model is represented as:

$$\begin{aligned} G(t)\dot{X}(t) - \dot{X}(t)Q(t) = q(&\frac{1}{2}\mathrm{sgn}^z(f_1(t)) \\ &+ \frac{1}{2}\mathrm{sgn}^{1/z}(f_1(t)) + j(\frac{1}{2}\mathrm{sgn}^z(f_2(t)) \\ &+ \frac{1}{2}\mathrm{sgn}^{1/z}(f_2(t)))) - \dot{G}(t)X(t) \\ &+ X(t)\dot{Q}(t) - \dot{S}(t). \end{aligned} \tag{9}$$

The IZNN model is represented as:

$$\begin{aligned} &G(t)\dot{X}(t) - \dot{X}(t)Q(t) \\ &\quad = q(\mathrm{sign}(f_1(t))(j_1|f_1(t)|^h \\ &\qquad + j_2|f_1(t)|^{1/h} - j_3|f_1(t)|) \\ &\qquad + j(\mathrm{sign}(f_2(t))(j_1|f_2(t)|^h \\ &\qquad + j_2|f_2(t)|^{1/h} - j_3|f_2(t)|))) - \dot{G}(t)X(t) \\ &\qquad + X(t)\dot{Q}(t) - \dot{S}(t), \end{aligned} \tag{10}$$

where $j_1 > j_3 > 0$, $j_2 > j_3 > 0$, and h is an odd integer and satisfy $h > 1$, and

$$\mathrm{sign}(u) = \begin{cases} 1, & \text{if } u > 0 \\ 0, & \text{if } u = 0 \\ -1, & \text{if } u < 0. \end{cases}$$

Now we can build a novel improved ZNN using the sign-multi-power function, which is designed as:

$$\begin{aligned} &G(t)\dot{X}(t) - \dot{X}(t)Q(t) \\ &\quad = q(a_1\mathrm{sgn}^z(f_1(t)) \\ &\qquad + a_2\mathrm{sgn}^{z-2^1}(f_1(t)) + a_3\mathrm{sgn}^{z-2^2}(f_1(t)) \\ &\qquad + \cdots + a_n\mathrm{sgn}^1(f_1(t)) + a_{n+1}\mathrm{sgn}^{1/z}(f_1(t)) \\ &\qquad + j(a_1\mathrm{sgn}^z(f_2(t)) + a_2\mathrm{sgn}^{z-2^1}(f_2(t)) \\ &\qquad + a_3\mathrm{sgn}^{z-2^2}(f_2(t)) + \cdots + a_n\mathrm{sgn}^1(f_2(t)) \\ &\qquad + a_{n+1}\mathrm{sgn}^{1/z}(f_2(t)))) - \dot{G}(t)X(t) \\ &\qquad + X(t)\dot{Q}(t) - \dot{S}(t), \end{aligned} \tag{11}$$

where $q > 0$, z is an odd integer and satisfies $z > 1$, $q > 0$, and the parameters $a_1, \cdots, a_{n+1}$ are all the positive numbers. We can call this model (11) as the ICZNN model.

C. THEOREM ANALYSIS OF ICZNN MODEL

Theorem 1: The ICZNN model (11) is globally stable no matter what its randomly generated initial value $X(0)$ is.

Proof: According to the error evolution (5), we can find each element of the matrix $D(t)$ has the same dynamics, then we have

$$\dot{D}_{iw}(t) = q\Psi(D_{iw}(t)), \tag{12}$$

where $D_{iw}(t)$ denotes the iwth element of the error matrix $D(t)$. According to $D_{iw}(t) = D_{iw,\mathrm{re}}(t) + jD_{iw,\mathrm{im}}(t)$, the following two real-valued equations are derived:

$$\begin{aligned} \dot{D}_{iw,\mathrm{re}}(t) &= q\Psi(D_{iw,\mathrm{re}}(t)), \\ \dot{D}_{iw,\mathrm{im}}(t) &= q\Psi(D_{iw,\mathrm{im}}(t)), \end{aligned} \tag{13}$$

where $D_{iw,\mathrm{re}}(t)$ and $D_{iw,\mathrm{im}}(t)$ denote the real part and imaginary part of $D_{iw}(t)$, respectively. Then we can design the following Lyapunov functions:

$$\begin{aligned} V_{\mathrm{re}}(t) &= D^2_{iw,\mathrm{re}}(t), \\ V_{\mathrm{im}}(t) &= D^2_{iw,\mathrm{im}}(t). \end{aligned} \tag{14}$$

Considering the equation $V_{\mathrm{re}}(t) = D^2_{iw,\mathrm{re}}(t)$ and the equation $V_{\mathrm{im}}(t) = D^2_{iw,\mathrm{im}}(t)$ have the identical dynamic, we need only take the equation $V_{\mathrm{re}}(t) = D^2_{iw,\mathrm{re}}(t)$ as a example to analyse the convergence property. Now we have

$$\dot{V}_{\mathrm{re}}(t) = -2qD_{iw,\mathrm{re}}(t)\Psi(D_{iw,\mathrm{re}}(t)). \tag{15}$$

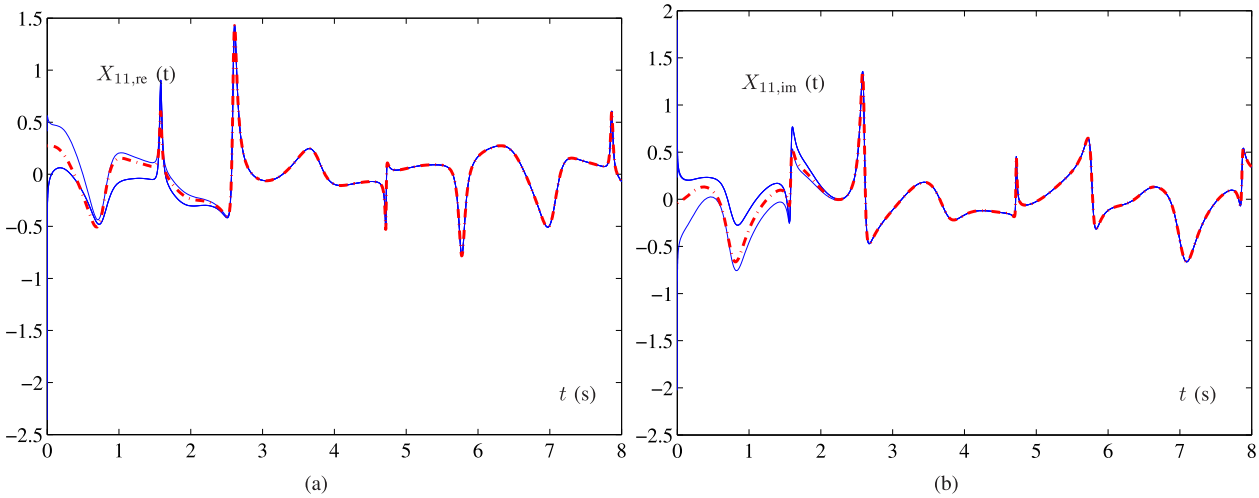

FIGURE 1. Output trajectories of neural states $X_{11}(t)$ synthesized by the model (9) in example 1.The dotted red line denotes the theoretical values, and the blue solid line denotes the calculated values. (a) Element of real part of $X_{11}(t)$. (b) Element of imaginary part of $X_{11}(t)$.

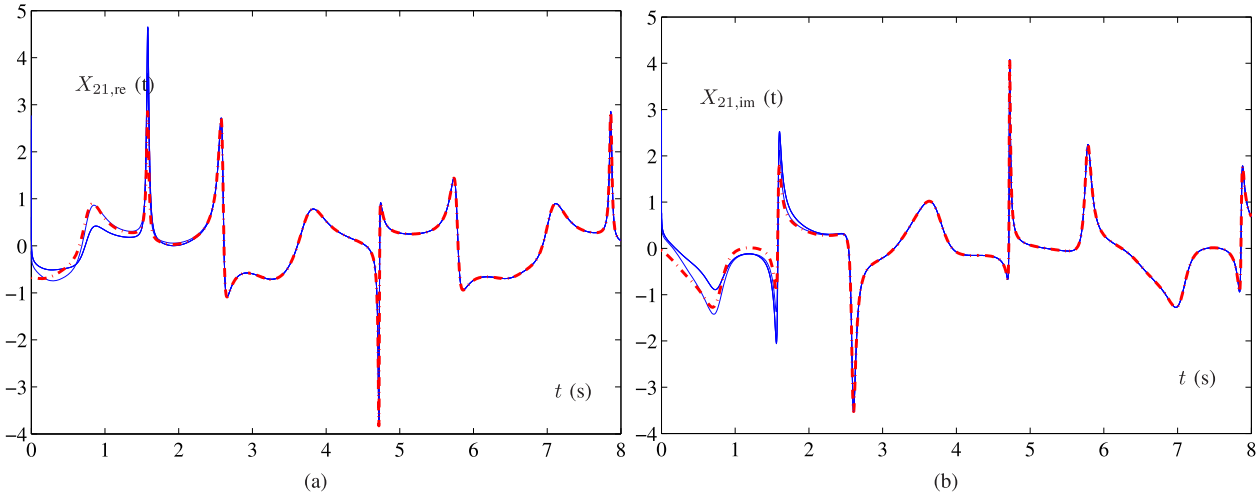

FIGURE 2. Output trajectories of neural states $X_{21}(t)$ synthesized by the model (9) in example 1. The dotted red line denotes the theoretical values, and the blue solid line denotes the calculated values. (a) Element of real part of $X_{21}(t)$. (b) Element of imaginary part of $X_{21}(t)$.

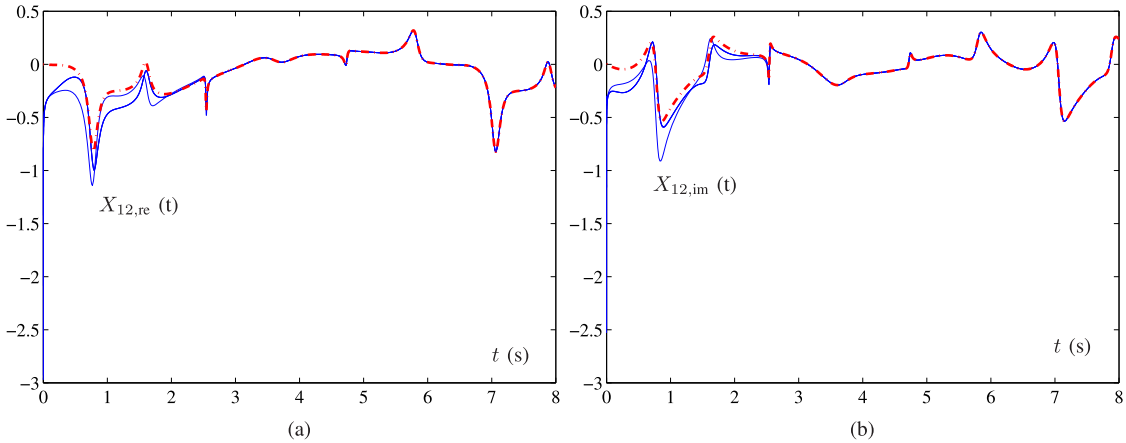

FIGURE 3. Output trajectories of neural states $X_{12}(t)$ synthesized by the model (9) in example 1. The dotted red line denotes the theoretical values, and the blue solid line denotes the calculated values. (a) Element of real part of $X_{12}(t)$. (b) Element of imaginary part of $X_{12}(t)$.

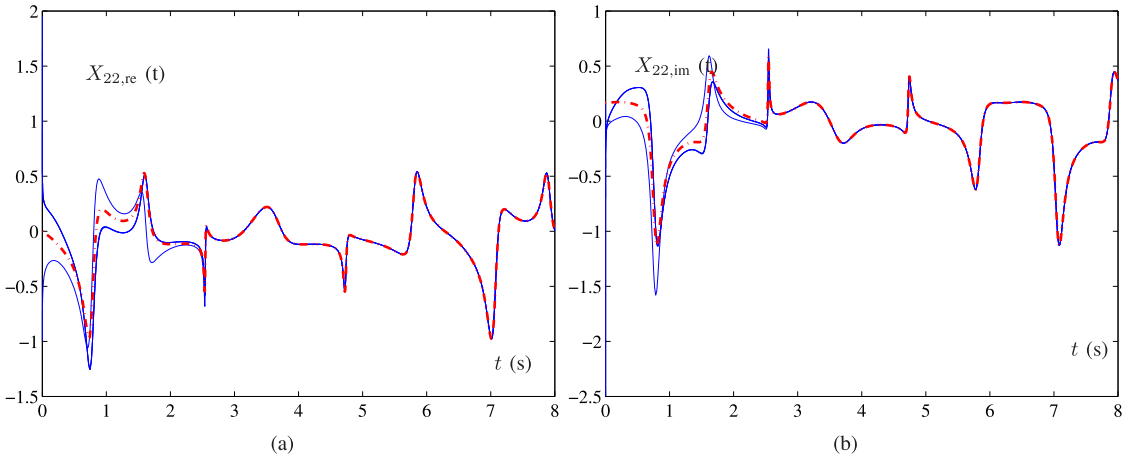

FIGURE 4. Output trajectories of neural states $X_{22}(t)$ synthesized by the model (9) in example 1. The dotted red line denotes the theoretical values, and the blue solid line denotes the calculated values. (a) Element of real part of $X_{22}(t)$. (b) Element of imaginary part of $X_{22}(t)$.

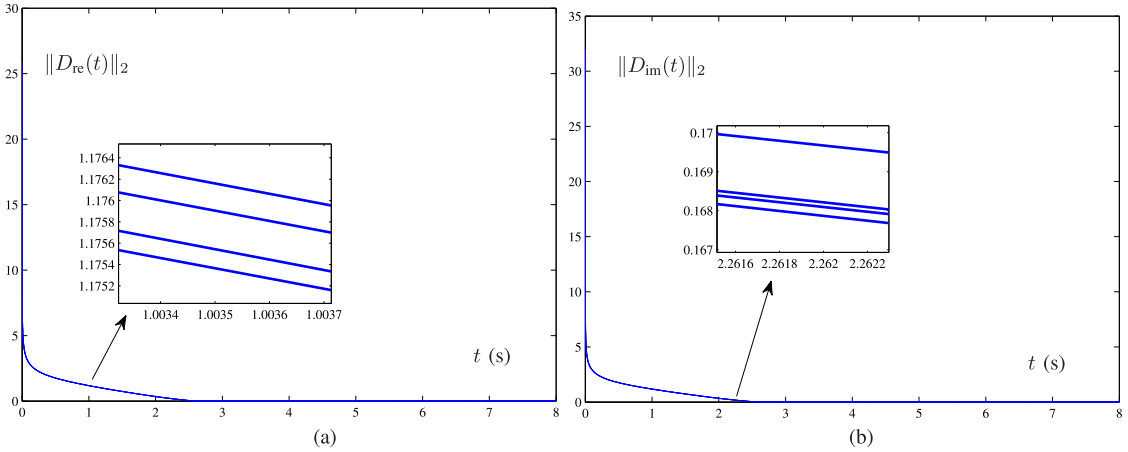

FIGURE 5. Output trajectories of the residual errors synthesized by the model (10) in example 1. (a) Element of real part of the residual errors, (b) Element of imaginary part of the residual errors.

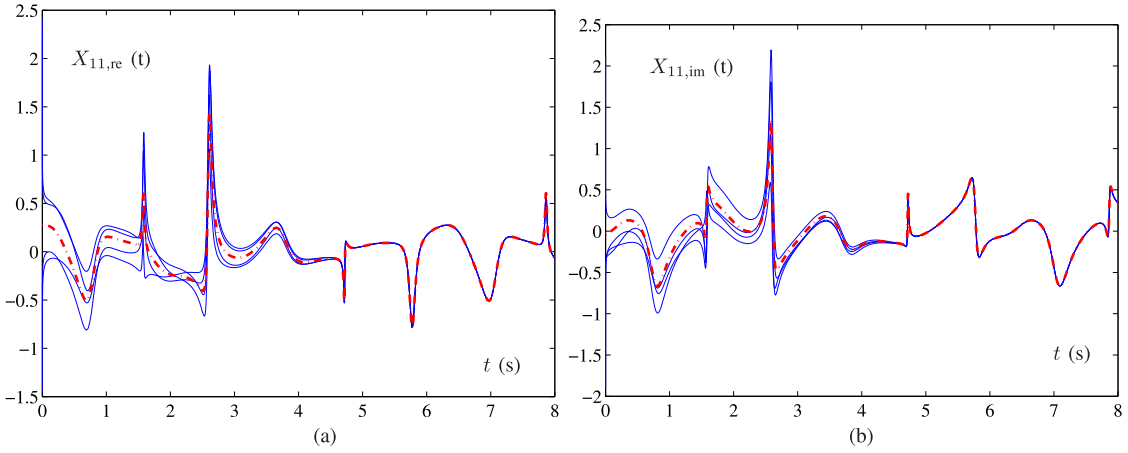

FIGURE 6. Output trajectories of neural states $X_{11}(t)$ synthesized by the model (10) in example 1. The dotted red line denotes the theoretical values, and the blue solid line denotes the calculated values. (a) Element of real part of the residual errors. (a) Element of real part of $X_{11}(t)$. (b) Element of imaginary part of $X_{11}(t)$.

If we choose the sign-multi-power activation function, we will have

$$\begin{aligned}\Psi(D_{iw,\mathrm{re}}(t)) = {} & a_1\mathrm{sgn}^{z}(D_{iw,\mathrm{re}}(t)) \\ & + a_2\mathrm{sgn}^{z-2^1}(D_{iw,\mathrm{re}}(t)) \\ & + a_3\mathrm{sgn}^{z-2^2}(D_{iw,\mathrm{re}}(t)) \\ & + \cdots + a_n\mathrm{sgn}^{1}(D_{iw,\mathrm{re}}(t)) \\ & + a_{n+1}\mathrm{sgn}^{1/z}(D_{iw,\mathrm{re}}(t)). \end{aligned} \tag{16}$$

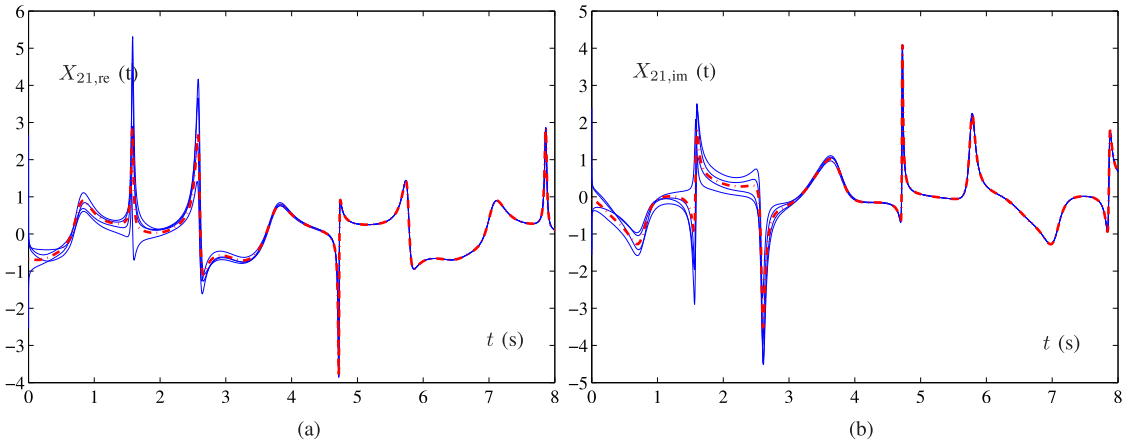

FIGURE 7. Output trajectories of neural states $X_{21}(t)$ synthesized by the model (10) in example 1. The dotted red line denotes the theoretical values, and the blue solid line denotes the calculated values. (a) Element of real part of $X_{21}(t)$. (b) Element of imaginary part of $X_{21}(t)$.

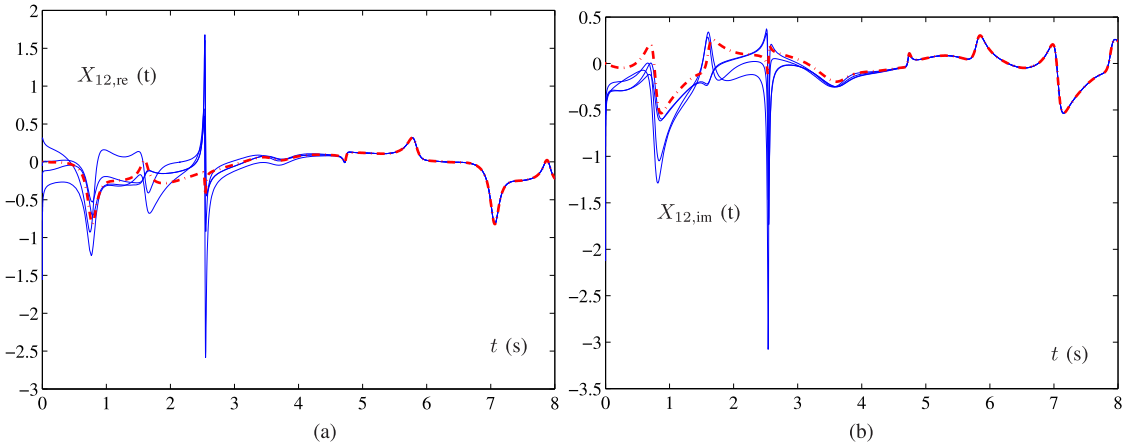

FIGURE 8. Output trajectories of neural states $X_{12}(t)$ synthesized by the model (10) in example 1. The dotted red line denotes the theoretical values, and the blue solid line denotes the calculated values. (a) Element of real part of $X_{12}(t)$. (b) Element of imaginary part of $X_{12}(t)$.

From the equation (16), we can first find $\mathrm{sgn}^{z}(t)$, $\cdots$ and $\mathrm{sgn}^{1/z}(t)$ are monotone increasing functions. Then the equation (16) is an odd and monotone increasing function. So $D_{iw,\mathrm{re}}(t)\Psi(D_{iw,\mathrm{re}}(t))$ is positive definite. Now according to the equation (15), $\dot{V}$ is negative definite. Then the corresponding conclusion can be given that $D_{iw,\mathrm{re}}(t)$ will converge to 0 globally with time for all i and w. Similarly, we can prove the convergence property of $D_{iw,\mathrm{im}}(t)$ for all i and w.

Now from the equation (4), the corresponding conclusions can be given that the $X(t)$ of the sign-multi-power model (11) will also converge to 0 globally. This proof is successful. ■

Theorem 2: The state $X(t)$ of ICZNN model (11) will obtain its theoretical solution within the time t_h:

$$t_h = \frac{z}{q(z-1)} V_{max}^{\frac{z-1}{2z}}(0)$$

where $V_{max}(0)$ denotes the maximum initial element of $D_{iw,\mathrm{re}}(t)$ and $D_{iw,\mathrm{im}}(t)$ for all possible i and w, and z is an odd integer and satisfy $z > 1$.

Proof: According to the equation (13), we first design the following Lyapunov function:

$$\begin{aligned} V_{\mathrm{re}}(t) &= D_{iw,\mathrm{re}}^2(t), \\ V_{\mathrm{im}}(t) &= D_{iw,\mathrm{im}}^2(t). \end{aligned} \tag{17}$$

Now we take the equation $V_{\mathrm{re}}(t) = D_{iw,\mathrm{re}}^2(t)$ as a example to analyse the maximum convergence time, and have

$$\begin{aligned} \dot{V}_{\mathrm{re}}(t) = & -2qD_{iw,\mathrm{re}}(t)(a_1\mathrm{sgn}^{z}(D_{iw,\mathrm{re}}(t)) \\ & + a_2\mathrm{sgn}^{z-2^1}(D_{iw,\mathrm{re}}(t)) + a_3\mathrm{sgn}^{z-2^2}(D_{iw,\mathrm{re}}(t)) \\ & + \cdots + a_n\mathrm{sgn}^{1}(D_{iw,\mathrm{re}}(t)) \\ & + a_{n+1}\mathrm{sgn}^{1/z}(D_{iw,\mathrm{re}}(t))) \\ = & -2q|D_{iw,\mathrm{re}}(t)|(a_1\mathrm{sgn}^{z}(|D_{iw,\mathrm{re}}(t)|) \\ & + a_2\mathrm{sgn}^{z-2^1}(|D_{iw,\mathrm{re}}(t)|) \\ & + a_3\mathrm{sgn}^{z-2^2}(|D_{iw,\mathrm{re}}(t)|) \\ & + \cdots + a_n\mathrm{sgn}^{1}(|D_{iw,\mathrm{re}}(t)|) \\ & + a_{n+1}\mathrm{sgn}^{1/z}(|D_{iw,\mathrm{re}}(t)|)) \end{aligned}$$

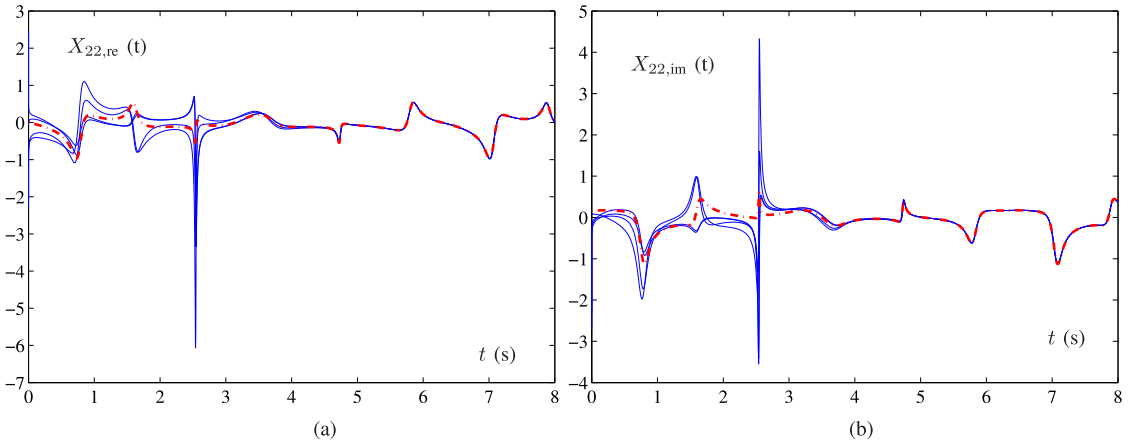

FIGURE 9. Output trajectories of neural states $X_{22}(t)$ synthesized by the model (10) in example 1. The dotted red line denotes the theoretical values, and the blue solid line denotes the calculated values. (a) Element of real part of $X_{22}(t)$. (b) Element of imaginary part of $X_{22}(t)$.

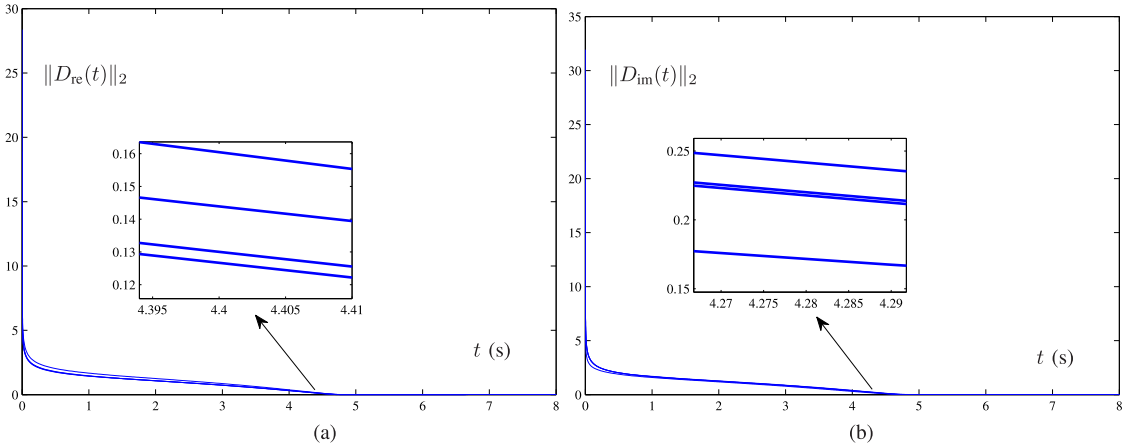

FIGURE 10. Output trajectories of the residual errors synthesized by the model (10) in example 1. (a) Element of real part of the residual errors. (b) Element of imaginary part of the residual errors.

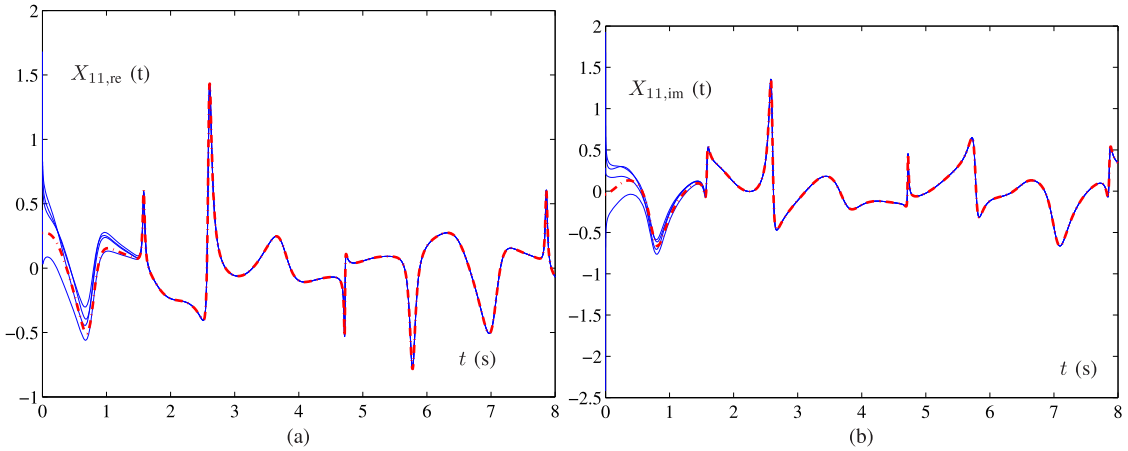

FIGURE 11. Output trajectories of neural states $X_{11}(t)$ synthesized by the model (11) in example 1. The dotted red line denotes the theoretical values, and the blue solid line denotes the calculated values. (a) Element of real part of $X_{11}(t)$. (b) Element of imaginary part of $X_{11}(t)$.

$$\leq -2q|D_{iw,\mathrm{re}}(t)|(a_{n+1}\mathrm{sgn}^{1/z}(|D_{iw,\mathrm{re}}(t)|))$$
$$= -2qV_{\mathrm{re}}{}^{1/2}(t)(a_{n+1}\mathrm{sgn}^{1/z}(V_{\mathrm{re}}{}^{1/2}(t))). \quad (18)$$

Then we have

$$\dot{V_{\mathrm{re}}}(t) \leq -2qV_{\mathrm{re}}{}^{1/2}(t)a_{n+1}\mathrm{sgn}^{1/z}(V_{\mathrm{re}}{}^{1/2}(t))$$

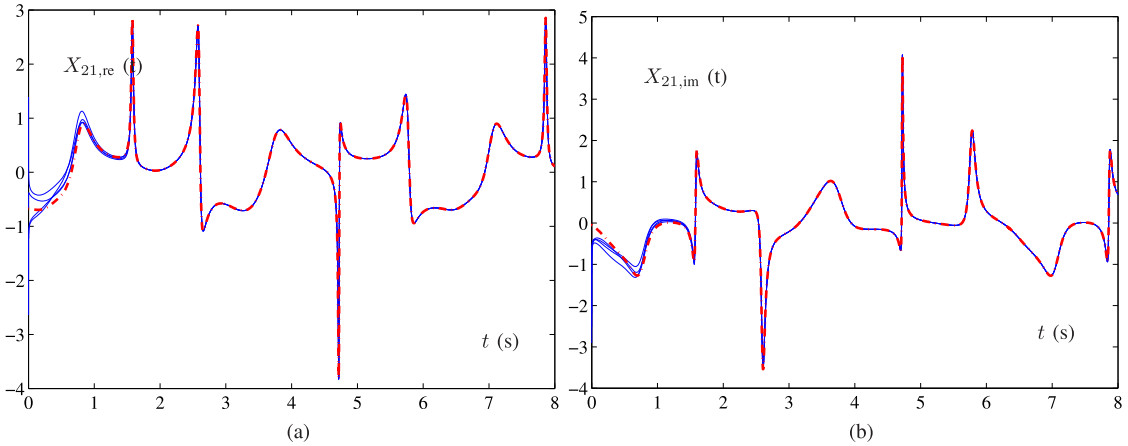

FIGURE 12. Output trajectories of neural states $X_{21}(t)$ synthesized by the model (11) in example 1. The dotted red line denotes the theoretical values, and the blue solid line denotes the calculated values. (a) Element of real part of $X_{21}(t)$. (b) Element of imaginary part of $X_{21}(t)$.

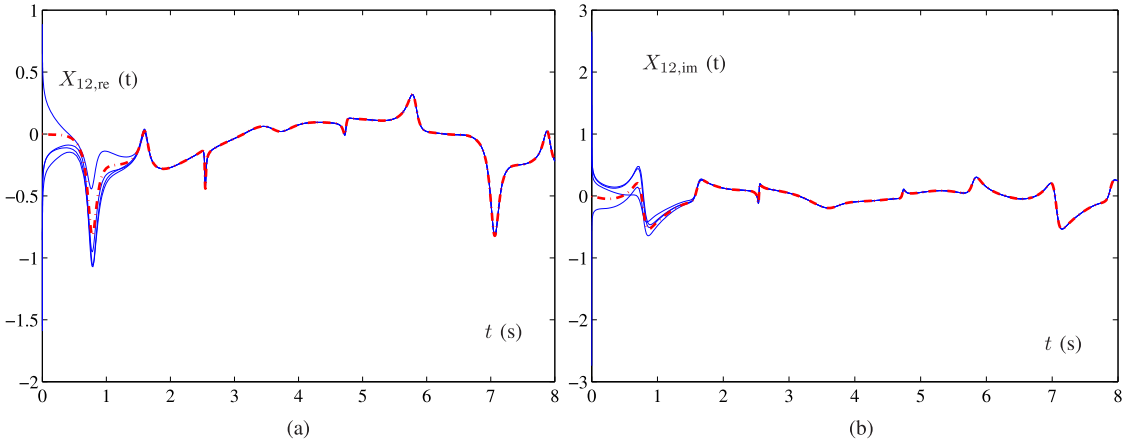

FIGURE 13. Output trajectories of neural states $X_{12}(t)$ synthesized by the model (11) in example 1. The dotted red line denotes the theoretical values, and the blue solid line denotes the calculated values. (a) Element of real part of $X_{12}(t)$. (b) Element of imaginary part of $X_{12}(t)$.

$$\begin{aligned} &= -2qV_{\mathrm{re}}{}^{1/2}(t)V_{\mathrm{re}}{}^{1/2z}(t) \\ &= -2qV_{\mathrm{re}}{}^{\frac{1+z}{2z}}(t). \end{aligned} \tag{19}$$

Now let's integrate the equation (19) from zero to t, and we will have

$$V_{\mathrm{re}}(t) \leq (V\mathrm{re}^{\frac{z-1}{2z}}(0) - \frac{q(z-1)}{z}t)^{\frac{2z}{z-1}}.$$

Let

$$t_{1,i} = \frac{z}{q(z-1)}v^{\frac{z-1}{2z}}(0). \tag{20}$$

Now we can draw a conclusion if $t \geq t_{1,i}$, $V_{\mathrm{re}}(t) = 0$. Suppose $V_{\mathrm{re},max}(0)$ denote the maximum element of $D_{iw,\mathrm{re}}(t)$ for all possible i and w, and $t_{1,\mathrm{re}} = \frac{z}{q(z-1)}V_{\mathrm{re},max}^{\frac{z-1}{2z}}(0)$. Therefore if $t \geq t_{1,\mathrm{re}}$, $V_{\mathrm{re}}(t) = 0$. Similarly, we can deal with the Lyapunov function $V_{\mathrm{im}}(t) = D_{iw,\mathrm{im}}^2(t)$ using the above method. Suppose $V_{\mathrm{im},max}(0)$ denote the maximum element of $D_{iw,\mathrm{im}}(t)$ for all possible i and w, and $t_{1,\mathrm{im}} = \frac{z}{q(z-1)}V_{\mathrm{im},max}^{\frac{z-1}{2z}}(0)$. Then we can find if $t \geq t_{1,\mathrm{im}}$, $V_{\mathrm{im}}(t) = 0$.

Suppose $t_1 = max(t_{1,\mathrm{re}}, t_{1,\mathrm{im}})$, and we can draw a conclusion that if $t \geq t_1$, the Lyapunov function (17) will converge to zero.

Now the proof is successful. ■

IV. NUMERICAL SIMULATION

Now, two illustrative examples are provided in this section. Furthermore to show the advantage of the ICZNN model (11), the sign-bi-power model (9) and the IZNN model (10) are also used to calculate the solution of CVTVSE. The convergence process of each neural-state solution and the residual error norm of each model are shown in corresponding figures. For the convenience of comparison, the following parameters are chosen $q = 1, z = h = 5, a_1 = a_2 = a_3 = a_4 = j_1 = j_2 = \frac{1}{2}$, and $j_3 = 0.25$.

Example 1: In this example, the sign-bi-power model (9), the IZNN model (10) and the ICZNN model (11) are employed to calculate the theoretical solution $\tilde{X}(t)$, respectively. The specific CVTVSE example is presented as below:

$$G_1(t)X(t) - X(t)Q_1(t) = -S_1(t) \in \mathbb{C}^{n\times n},$$

where

$$G_1 = \begin{bmatrix} \cos(5t) + j4\sin(2t) & 3\sin(4t) + j6\cos(3t) \\ 6 - \sin(t) + j\cos(4t) & 2 + \cos(2t) + j3\sin(2t) \end{bmatrix},$$

$$Q_1 = \begin{bmatrix} 2 & 0 \\ 0 & 3 \end{bmatrix},$$

and

$$S_1 = \begin{bmatrix} \sin(3t) & \sin(2t) \\ -\cos(t) + j4\sin(3t) & \sin(t) \end{bmatrix}.$$

The calculation results are displayed in Figs.1-15. The Figs. 1-4, the Figs. 6-9 and the Figs. 11-14 display the output trajectories of neural state $X(t)$. From these figures, we can find that the complex-valued time-varying parameters $X_{11}(t)$, $X_{21}(t)$, $X_{12}(t)$, $X_{22}(t)$ of different models will all converge to the theoretical solution in finite time. However, the ICZNN model (11) has the highest convergence speed. The Fig. 5, the Fig. 10 and the Figs. 15-18 display the output trajectories of the residual error norm $||D(t)||_2$. From these figures, we can find that the convergence time of the sign-bi-power model (9), the IZNN model (10), and the ICZNN model (11) is about 2.6s, 4.7s, and 1.7s, respectively. Compared with the sign-bi-power model (9) and the IZNN model (10), the ICZNN model increases the convergence speed about percent 34% and 62%, respectively.

Example 2: In this example, the sign-bi-power model (9), the IZNN model (10) and the sign-multi-power model (11) are further employed to calculate the following CVTVSE:

$$G_2(t)X(t) - X(t)Q_2(t) = -S_2(t) \in \mathbb{C}^{n\times n},$$

where

$$G_2 = p\begin{bmatrix} \cos(t) + j3\sin(4t) & 5\sin(3t) + j\cos(4t) \\ 8 - j\cos(4t) & 6\cos(3t) + j\sin(4t) \end{bmatrix},$$

$$Q_2 = \begin{bmatrix} 2 + j\cos(2t) & 4 + j\sin(3t) \\ \cos(3t) - j\sin(2t) & 3 + \cos(t) \end{bmatrix},$$

and

$$S_2 = \begin{bmatrix} \sin(t) + j4\cos(t) & \cos(t) \\ -\cos(t) + j\sin(3t) & \sin(t) + j\sin(2t) \end{bmatrix}.$$

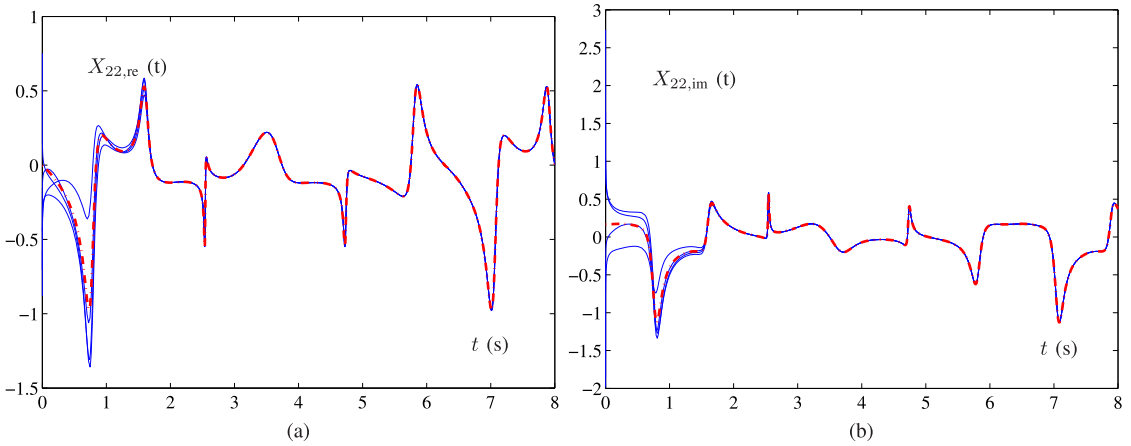

FIGURE 14. Output trajectories of neural states $X_{22}(t)$ synthesized by the model (11) in example 1. The dotted red line denotes the theoretical values, and the blue solid line denotes the calculated values. (a) Element of real part of $X_{22}(t)$. (b) Element of imaginary part of $X_{22}(t)$.

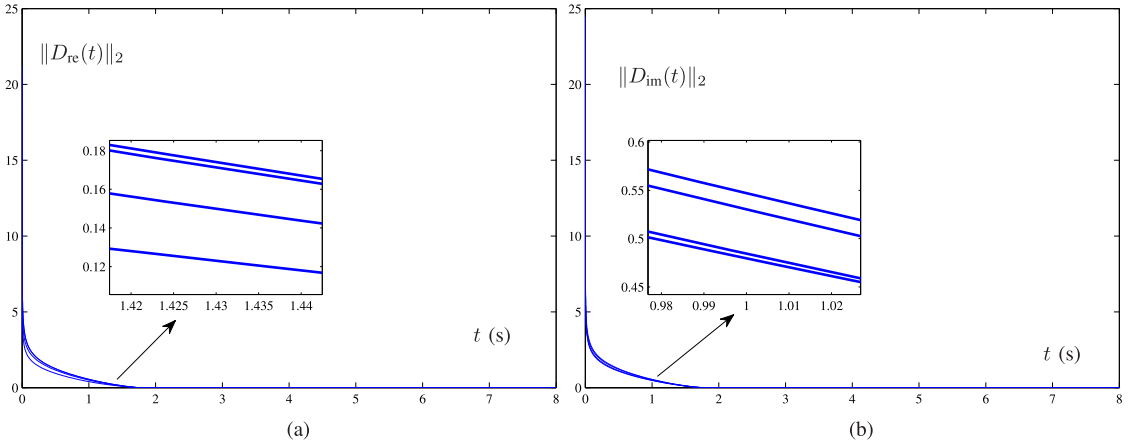

FIGURE 15. Output trajectories of the residual errors synthesized by the model (11) in example 1. (a) Element of real part of the residual errors. (b) Element of imaginary part of the residual errors.

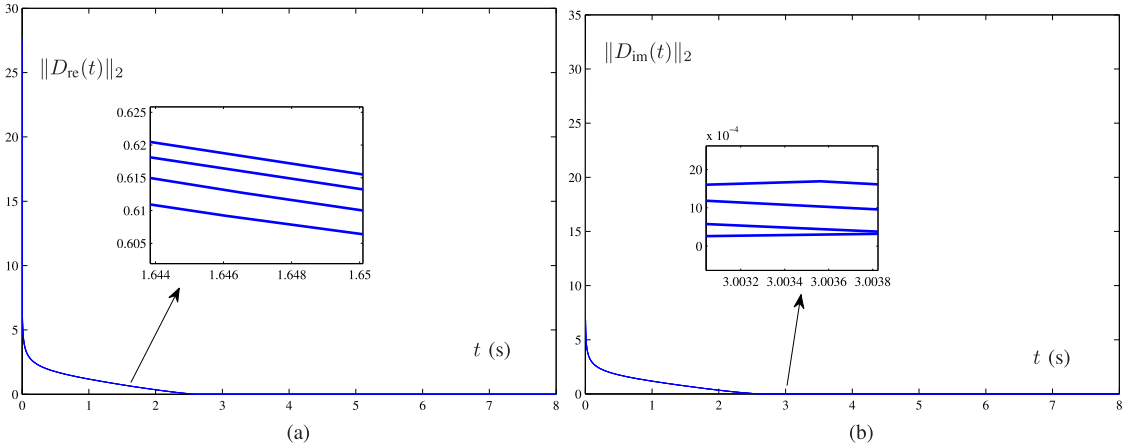

FIGURE 16. Output trajectories of the residual errors synthesized by the model (9) in example 2. (a) Element of real part of the residual errors. (b) Element of imaginary part of the residual errors.

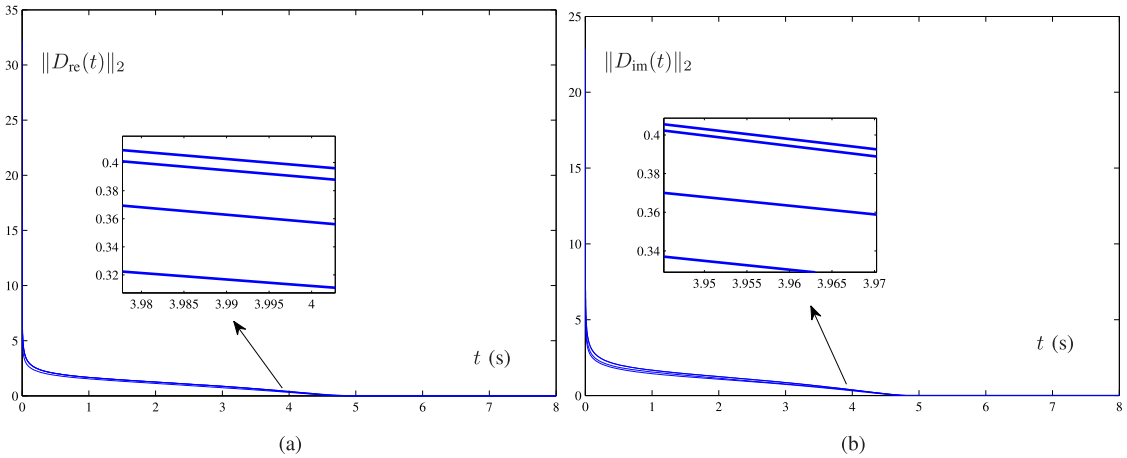

FIGURE 17. Output trajectories of the residual errors synthesized by the model (10) in example 2. (a) Element of real part of the residual errors. (b) Element of imaginary part of the residual errors.

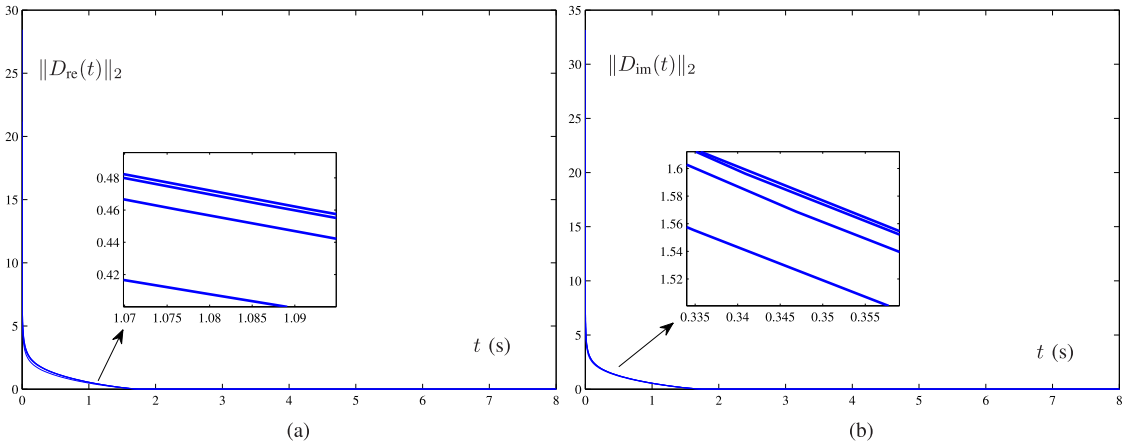

FIGURE 18. Output trajectories of the residual errors synthesized by the model (11) in example 2. (a) Element of real part of the residual errors. (b) Element of imaginary part of the residual errors.

The calculation results are displayed in Fig.16-18 which show the output trajectories of the residual error norm $||D(t)||_2$. Similarly, we can find the the sign-multi-power model (11) has a higher convergence speed than the sign-bi-power model (9) and the IZNN model (10).

V. CONCLUSIONS

In this paper a novel activation function is designed. Based on this novel activation function, a new finite-time ZNN model (11) is designed to tackle the CVTVSE, and the strict proof of global convergence and the upper bound are described. The simulation results validate the proposed ICZNN model can increase the convergence speed significantly. So it has a certain significance for tackling the CVTVSE online.

REFERENCES

[1] L. Xiao, Z. Zhang, Z. Zhang, W. Li, and S. Li, "Design, verification and robotic application of a novel recurrent neural network for computing dynamic Sylvester equation," *Neural Netw.*, vol. 105, pp. 185–196, Sep. 2018.

[2] E. Ringh, G. Mele, J. Karlsson, and E. Jarlebring, "Sylvester-based preconditioning for the waveguide eigenvalue problem," *Linear Algebra Appl.*, vol. 542, pp. 441–463, Apr. 2018.

[3] S. Chen and Y. Tian, "On T-Sylvester equations over commutative rings," *J. Franklin Inst.*, vol. 353, no. 5, pp. 1102–1108, 2016.

[4] G. Sangalli and M. Tani, "Isogeometric preconditioners based on fast solvers for the Sylvester equation," *SIAM J. Sci. Comput.*, vol. 38, no. 6, pp. 1–28, 2016.

[5] A. Mesbahi and J. M. Velni, "Distributed observer-based cooperative control for output regulation in multi-agent linear parameter-varying systems," *IET Control Theory Appl.*, vol. 11, no. 9, pp. 1394–1403, 2017.

[6] R. H. Bartels and G. W. Stewart, "Solution of the matrix equation AX + XB = C [F4]," *Commun. ACM*, vol. 15, no. 9, pp. 820–826, Sep. 1972.

[7] G. H. Golub, S. Nash, and C. Van Loan, "A Hessenberg–Schur method for the problem AX + XB = C," *IEEE Trans. Autom. Contr.*, vol. 24, no. 6, pp. 909–913, Dec. 1979.

[8] X. Sheng, "A relaxed gradient based algorithm for solving generalized coupled Sylvester matrix equations," *J. Franklin Inst.*, vol. 355, no. 10, pp. 4282–4297, 2018.

[9] F. Ding and T. Chen, "Iterative least-squares solutions of coupled Sylvester matrix equations," *Syst. Control Lett.*, vol. 54, no. 2, pp. 95–107, Feb. 2015.

[10] Y.-J. Xie and C.-F. Ma, "The accelerated gradient based iterative algorithm for solving a class of generalized Sylvester-transpose matrix equation," *Appl. Math. Comput.*, vol. 273, pp. 1257–1269, Jan. 2016.

[11] G. M. Flagg and S. Gugercin, "On the ADI method for the Sylvester equation and the optimal-H_2 points," *Appl. Numer. Math.*, vol. 64, pp. 50–58, Feb. 2013.

[12] T. Gao, Y.-J. Liu, L. Liu, and D. Li, "Adaptive neural network-based control for a class of nonlinear pure-feedback systems with time-varying full state constraints," *IEEE/CAA J. Automatica Sinica*, vol. 5, no. 5, pp. 923–933, Sep. 2018.

[13] L. Liu, Y.-J. Liu, and S. Tong, "Fuzzy based multi-error constraint control for switched nonlinear systems and its applications," *IEEE Trans. Fuzzy Syst.*, to be published. doi: 10.1109/TFUZZ.2018.2882173.

[14] D.-P. Li and D.-J. Li, "Adaptive neural tracking control for an uncertain state constrained robotic manipulator with unknown time-varying delays," *IEEE Trans. Syst., Man, Cybern. Syst.*, vol. 48, no. 12, pp. 2219–2228, Dec. 2018. doi: 10.1109/TSMC.2017.2703921.

[15] Y. Zhang and S. S. Ge, "Design and analysis of a general recurrent neural network model for time-varying matrix inversion," *IEEE Trans. Neural Netw.*, vol. 16, no. 6, pp. 1477–1490, Nov. 2005.

[16] C. Yi, Y. Chen, and X. Lan, "Comparison on neural solvers for the Lyapunov matrix equation with stationary nonstationary coefficients," *Appl. Math. Model.*, vol. 37, no. 4, pp. 2495–2502, Feb. 2013.

[17] D. Chen, S. Li, and Q. Wu, "Rejecting chaotic disturbances using a super-exponential-zeroing neurodynamic approach for synchronization of chaotic sensor systems," *Sensors*, vol. 19, no. 1, p. 74, 2019.

[18] D. Chen, Y. Zhang, and S. Li, "Tracking control of robot manipulators with unknown models: A Jacobian-matrix-adaption method," *IEEE Trans. Ind. Informat.*, vol. 14, no. 7, pp. 3044–3053, Jul. 2018.

[19] L. Liu, Y.-J. Liu, and S. Tong, "Neural networks-based adaptive finite-time fault-tolerant control for a class of strict-feedback switched nonlinear systems," *IEEE Trans. Cybern.*, to be published. doi: 10.1109/TCYB.2018.2828308.

[20] L. Liu, Z. Wang, and H. Zhang, "Neural-network-based robust optimal tracking control for MIMO discrete-time systems with unknown uncertainty using adaptive critic design," *IEEE Trans. Neural Netw. Learn. Syst.*, vol. 29, no. 4, pp. 1239–1251, Apr. 2018.

[21] L. Liu, Y.-J. Liu, and S. Tong, "Fuzzy based multi-error constraint control for switched nonlinear systems and its applications," *IEEE Trans. Fuzzy Syst.*, to be published. doi: 10.1109/TFUZZ.2018.2882173.

[22] F. Ding and T. Chen, "Gradient based iterative algorithms for solving a class of matrix equations," *IEEE Trans. Autom. Control*, vol. 50, no. 8, pp. 1216–1221, Aug. 2005.

[23] B. Zhou, Z.-Y. Li, G.-R. Duan, and Y. Wang, "Weighted least squares solutions to general coupled Sylvester matrix equations," *J. Comput. Appl. Math.*, vol. 224, no. 2, pp. 759–776, Feb. 2009.

[24] L. Jin and Y. Zhang, "Discrete-time Zhang neural network for online time-varying nonlinear optimization with application to manipulator motion generation," *IEEE Trans. Neural Netw. Learn. Syst.*, vol. 26, no. 7, pp. 1525–1531, Jul. 2015.

[25] D. Guo, Z. Nie, and L. Yan, "Novel discrete-time Zhang neural network for time-varying matrix inversion," *IEEE Trans. Syst., Man, Cybern., Syst.*, vol. 47, no. 8, pp. 2301–2310, Aug. 2017.

[26] L. Xiao, B. Liao, S. Li, Z. Zhang, L. Ding, and L. Jin, "Design and analysis of FTZNN applied to the real-time solution of a nonstationary Lyapunov equation and tracking control of a wheeled mobile manipulator," *IEEE Trans. Ind. Informat.*, vol. 14, no. 1, pp. 98–105, Jan. 2018.

[27] L. Jin, S. Li, X. Luo, and Y. Li, "Neural dynamics for cooperative control of redundant robot manipulators," *IEEE Trans. Ind. Informat.*, vol. 14, no. 9, pp. 3812–3821, Sep. 2018. doi: 10.1109/TII.2018.278943.

[28] L. Jin, Y. Zhang, S. Li, and Y. Zhang, "Modified ZNN for time-varying quadratic programming with inherent tolerance to noises and its application to kinematic redundancy resolution of robot manipulators," *IEEE Trans. Ind. Electron.*, vol. 63, no. 11, pp. 6978–6988, Nov. 2016.

[29] L. Jin and S. Li, "Nonconvex function activated zeroing neural network models for dynamic quadratic programming subject to equality and inequality constraints," *Neurocomputing*, vol. 267, pp. 107–113, Dec. 2017.

[30] L. Xiao, "A new design formula exploited for accelerating Zhang neural network and its application to time-varying matrix inversion," *Theor. Comput. Sci.*, vol. 647, pp. 50–58, Sep. 2016.

[31] Y. Zhang, Y. Ding, B. Qiu, Y. Zhang, and X. Li, "Signum-function array activated ZNN with easier circuit implementation and finite-time convergence for linear systems solving," *Inf. Process. Lett.*, vol. 124, pp. 30–34, Aug. 2017.

[32] L. Xiao, "Accelerating a recurrent neural network to finite-time convergence using a new design formula and its application to time-varying matrix square root," *J. Franklin Inst.*, vol. 354, no. 13, pp. 5667–5677, 2017.

[33] S. Qiao, X.-Z. Wang, and Y. Wei, "Two finite-time convergent Zhang neural network models for time-varying complex matrix Drazin inverse," *Linear Algebra Appl.*, vol. 542, pp. 101–117, Apr. 2018.

[34] L. Xiao, "A finite-time recurrent neural network for solving online time-varying Sylvester matrix equation based on a new evolution formula," *Nonlinear Dyn.*, vol. 90, no. 3, pp. 1581–1591, 2017.

[35] Y. Shen, P. Miao, Y. Huang, and Y. Shen, "Finite-time stability and its application for solving time-varying Sylvester equation by recurrent neural network," *Neural Process. Lett.*, vol. 42, no. 3, pp. 763–784, 2015.

[36] Y.-J. Huang, X.-Y. Wang, H.-X. Long, and X.-H. Yang, "Synthesization of high-capacity auto-associative memories using complex-valued neural networks," *Chin. Phys. B*, vol. 25, no. 12, 2016, Art. no. 120701.

[37] K. Ichikawa and A. Hirose, "Singular unit restoration in InSAR using complex-valued neural networks in the spectral domain," *IEEE Trans. Geosci. Remote Sens.*, vol. 55, no. 3, pp. 1717–1723, Mar. 2017.

[38] Y. Arima and A. Hirose, "Performance dependence on system parameters in millimeter-wave active imaging based on complex-valued neural networks to classify complex texture," *IEEE Access*, vol. 5, pp. 22927–22939, 2017.

[39] M. Che, L. Qi, Y. Wei, and G. Zhang, "Geometric measures of entanglement in multipartite pure states via complex-valued neural networks," *Neurocomputing*, vol. 313, pp. 25–38, Nov. 2018.

[40] Y. Zhang, Z. Li, and K. Li, "Complex-valued Zhang neural network for online complex-valued time-varying matrix inversion" *Appl. Math. Comput.*, vol. 217, no. 24, pp. 10066–10073, 2011.

[41] S. Li, S. Chen, and B. Liu, "Accelerating a recurrent neural network to finite-time convergence for solving time-varying Sylvester equation by using a sign-bi-power activation function," *Neural Process. Lett.*, vol. 37, no. 2, pp. 189–205, 2013.
[42] S. Li and Y. Li, "Nonlinearly activated neural network for solving time-varying complex Sylvester equation," *IEEE Trans. Cybern.*, vol. 44, no. 8, pp. 1397–1407, Aug. 2014.
[43] P. Miao, Y. Shen, Y. Huang, and Y.-W. Wang, "Solving time-varying quadratic programs based on finite-time Zhang neural networks and their application to robot tracking," *Neural Comput. Appl.*, vol. 26, no. 3, pp. 693–703, Apr. 2015.
[44] L. Ding, L. Xiao, K. Zhou, Y. Lan, and Y. Zhang, "A new RNN model with a modified nonlinear activation function applied to complex-valued linear equations," *IEEE Access*, vol. 6, pp. 62954–62962, 2018.

LEI DING received the Ph.D. degree in control science and engineering from Central South University, Changsha, China, in 2009. He is currently a Professor with the College of Information Science and Engineering, Jishou University, Jishou, China. His main research interests include neural networks, network security, and intelligent computing.

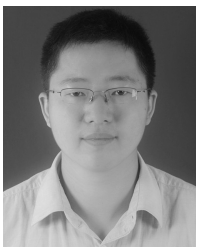

LIN XIAO received the B.S. degree in electronic information science and technology from Hengyang Normal University, Hengyang, China, in 2009, and the Ph.D. degree in communication and information systems from Sun Yat-sen University, Guangzhou, China, in 2014. He is currently an Associate Professor with the College of Information Science and Engineering, Jishou University, Jishou, China. His main research interests include neural networks, robotics, and intelligent information processing.

KAIQING ZHOU received the B.S. degree in computer science and technology from Jishou University, in 2006, the M.S. degree in computer applied techniques from the Changsha University of Science and Technology, in 2011, and the Ph.D. degree in computer science from Universiti Teknologi Malaysia, in 2016. He is currently a Lecturer with the Department of Data Science and Big Data Technology, College of Information and Engineering, Jishou University. He is also a Postdoctoral Fellow with the College of Information and Engineering, Central South University. His main research interests include fuzzy Petri net and its applications, Chinese information process, and soft computing techniques.

YONGHONG LAN received the B.S. and M.S. degrees in applied mathematics from Xiangtan University, Xiangtan, China, in 1999 and 2004, respectively, and the Ph.D. degree in control theory and control engineering from Central South University, Changsha, China, in 2010. He is currently a Professor with the School of Information Engineering, Xiangtan University, Xiangtan, China. His current research interests are fractional order control systems and iterative learning control.

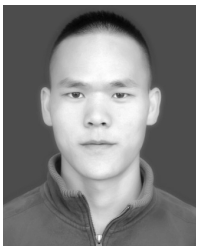

YONGSHENG ZHANG received the B.S. degree from Jishou University, Jishou, China, in 2017, where he is currently pursuing the Ph.D. degree with the College of Information Science and Engineering. His main research interests include neural networks and robotics.

JICHUN LI received the B.S. and M.S. degrees in mechatronic engineering from the China University of Geosciences, Wuhan, China, in 2000 and 2003, respectively, and the Ph.D. degree in mechanical engineering from King's College London, University of London, U.K., in 2013. He is currently a Lecturer/Senior Lecturer with the Department of Engineering, School of Science, Engineering and Design, Teesside University. His main research interests include medical devices, electric car battery, not-destructive testing, operational management and intelligent transportation, the IoT, and AI solutions for bespoke robotics in chemical, environmental, life science, energy, and agri-food industries. He is a member of the IEEE, IET, and IMeChE.